

Achieving Exceptional Mechanical and Thermal Properties in ABS/MWCNTs Nanocomposites with Minimal CNT Loading via Electromechanical Dispersion Technique (EMDT)

Ayub KarimzadGhavidel¹, Tahsin Tecelli Opoz², Mahsa Mahdavinia¹, Gholamreza Kiani¹, Mahmoud Moradi^{4*}

¹ Department of Mechanical Engineering, National University of Skills (NUS), Tehran 1435761137, Iran

² General Engineering Research Institute, School of Engineering, Liverpool John Moores University,
Liverpool L33AF, UK

³ Department of Organic Chemistry and Biochemistry, Faculty of Chemistry, University of Tabriz, Tabriz
5166616471, Iran

⁴ Faculty of Arts, Science and Technology, University of Northampton, Northampton NN1 5PH, UK

mahmoud.moradi@northampton.ac.uk

Abstract

This research aims to decrease the concentration of carbon nanotubes (CNTs) needed for enhancing the mechanical and thermal properties of acrylonitrile butadiene styrene (ABS)/CNTs nanocomposites using the recently introduced Electromechanically-Dispersion Technique (EMDT). EMDT efficiently disperses CNTs' agglomerations, preventing structural damage. Nanocomposites with various CNTs concentration were produced with EMDT, followed by injection molding to provide tensile strength, thermal conductivity, and impact resistance samples. Raman and differential scanning calorimetry (DSC) assessed CNTs dispersion, revealing successful dispersion up to 0.2 wt.% without structural damage. At this concentration, the tensile strength improved to 47.08 MPa, showing an increase of approximately 17.5%, and the thermal conductivity significantly increased to 0.29 W/mK, reflecting a 46% improvement. These results surpass those achieved by traditional dispersion methods, where 10 times the CNT concentration was required to reach similar enhancements. Higher injection temperatures and holding pressures improved CNTs alignment and reduced

entanglement, enhancing properties. However, no additional improvements were observed beyond 0.2 wt.%. These findings highlight EMDT's potential in creating high-performance nanocomposites with significantly lower CNTs concentrations.

Highlights

- Utilization of the novel EMDT dispersion method in nanocomposite preparation
- Overcoming hindrances to commercialize CNT-based polymeric nanocomposites
- Reducing the required CNTs concentration to attain significant properties
- Improving tensile strength of ABS by ~17.5% with just 0.2 wt.% of CNTs
- Remarkable 48.4% increase in ABS thermal conductivity with just 0.2 wt.% of CNTs

Keywords: Electromechanically-Dispersed Technique (EMDT)/ Melt mixing/ CNTs/Dispersion/ Acrylonitrile Butadiene Styrene (ABS).

1. Introduction

Polymer-based nanocomposites hold a distinct position in the modern world due to their exceptional characteristics [1, 2]. Within this domain, carbon nanotubes have garnered considerable attention as fillers for their capacity to simultaneously enhance mechanical, thermal, and electrical properties of polymers [3, 4]. This prominence has facilitated the industrial-scale production of these nanoparticles [5, 6]. A challenging aspect associated with these nanoparticles is the strong van der Waals force between them, resulting in the creation of bundles and agglomerations [7, 8]. Consequently, an efficient process is imperative for their separation and dispersion [9]. For this purpose, several methods focus on the utilization of high shearing force, including ultrasonic waves on a laboratory scale or the extruder process for industrial applications [10, 11]. Each method comes with its own advantages and disadvantages, which will be discussed below.

In the mass-production approach adopted by industries, the creation of nanocomposite granules and their subsequent transformation into parts involves three main stages: pre-

mixing, melt mixing (extrusion), and the forming process [12, 13]. Stage (I), Pre-mixing encompasses mechanical blending, physically combining nanoparticles with pure polymer granules [14, 15]. This step presents a challenge during the extrusion process [13], primarily due to the size difference between polymer granules and nanoparticles, leading to difficulty in achieving a homogenous mixture for melt mixing [16]. To achieve uniform blending, researchers have employed various techniques, including granule crushing and size adjustment to align with nanoparticle agglomerations [17]. However, in the case of compounds containing carbon nanotubes (CNTs), this step has limited impact on agglomeration size [17]. Another explored approach at this stage involves creating a CNT suspension through ball milling with a solvent, followed by dissolving polymeric granules in this solution [12, 18]. Noteworthy is the focus of this method on fragmenting CNTs via ball milling. An important consideration with this approach is the potential fragmentation, structural damage, and shortening of CNT lengths caused by the milling balls [19].

Stage (II) involves melt mixing, where the mixture prepared in step (I) undergoes processing using an extruder to generate nanocomposite granules. Throughout this operation, the nanotubes undergo significant damage and experience a substantial reduction in length due to the application of high shearing force [20]. Conversely, the most notable attribute of nanotubes that has garnered considerable attention is their aspect ratio, denoting the ratio of their length to their outside diameter [21]. The significance of this characteristic is further underscored when dealing with nanocomposites aiming to enhance mechanical strength, thermal conductivity, and electrical conductivity simultaneously. Therefore, it is of utmost importance for the aspect ratio to remain as close to its initial value as possible [22]. Despite the mentioned drawbacks of the extrusion process, it continues to be one of the primary methods for industrial-scale nanocomposite production due to its capacity to achieve high production volumes efficiently and cost-effectively [22].

Stage (III), Nanocomposite granules produced through extrusion are mainly employed in the manufacturing of industrial and practical parts using the injection molding method. This process, similar to extrusion, not only negatively impacts the structure of CNTs but also leads to their partial orientation and agglomeration during the injection process [23], thereby significantly influencing the mechanical, electrical, and thermal properties of CNTs [22].

A novel method called Electro-Mechanically Dispersion Technique (EMDT) has recently been developed to disperse CNTs within a liquid medium, relying on the electric field to align the CNTs [23]. The high-frequency variation in the electric field leads to the reorientation and vibration of CNT agglomerates, while the surrounding fluid applies stress on the CNTs, ultimately causing the disentanglement of the CNTs. In this method, the amount of applied stress is not high enough to damage the CNTs' structure, nor is it sufficient to separate the CNTs directly. However, the frequency of the applied shear stress induces a mechanical fatigue phenomenon between CNT-CNT van-der-Waals interactions, which consequently leads to their dispersion. Therefore, unlike traditional dispersion methods that subject CNTs to considerable shear forces, EMDT shifts the mechanism from dispersion by high shear force to mechanical fatigue, allowing it to preserve the length and structure of the nanotubes [23]. Moreover, EMDT is an energy-efficient process that requires significantly lower operational energy compared to high-energy techniques, eliminating the need for prolonged ultrasonication or high-temperature processing. Operating at room temperature, it employs environmentally friendly processing conditions, making it a sustainable approach that aligns with green manufacturing practices and industrial scalability goals [23].

For the first time, this study applies EMDT to produce ABS/CNT nanocomposites, followed by injection molding. This approach enables investigation of the combined influence of EMDT and key injection molding parameters on the mechanical and thermal properties of the nanocomposites. Specifically, the effects of CNT concentration, molding temperature, and holding pressure are considered as variables, each carefully examined. It is expected that this novel dispersion method, by protecting CNTs' structure and length and considering key EMDT parameters under optimal conditions, will reduce excessive CNT concentrations traditionally required, achieving unprecedented improvements in mechanical and thermal properties.

2. Materials and Methods

2.1. Materials

The multi-walled carbon nanotubes (MWCNTs) synthesized through the process of chemical vapor deposition (CVD) were purchased from NanoAmor (Texas, US). These MWCNTs

possess an outer diameter (OD) ranging from 30 to 50 nm, an inner diameter (ID) ranging from 5 to 15 nm, a length of 10 to 20 μm , a purity exceeding 95%, a density of 2.1 g/cm^3 , an aspect ratio ranging from 200 to 666, and a surface area from 90 to 120 m^2/g .

As for the polymer matrix, ABS graft phases with butadiene and styrene acrylonitrile (SAN) in powdered form were utilized (SV0157-Tabriz Petrochemical Co). The polymer matrix underwent extrusion and was subsequently transformed into granules. The average sizes of the SAN phase and polybutadiene (PB) phase are 100 μm and 200 μm , respectively. A microscopic depiction of this powder can be found in the Supplementary Information section, specifically in **Figure S1**, along with its detailed characteristics tabulated in **Table S1**.

2.2. Specimens and Fabrication Method

First, both the CNTs and the polymer matrix were dried at 85 $^{\circ}\text{C}$ for a duration of 2 hours within an oven. Following this, they were combined at varying concentrations of 0.1%, 0.2%, and 0.3 wt.% of CNTs. The mixture was then placed into one-third of a 3-Liter jar. Subsequently, the jar was positioned onto a ball milling machine and processed for a duration of 12 hours at a speed of 60 rpm. The unfilled section of the jar was deliberately left open to facilitate unimpeded movement of the materials within, thereby promoting collisions between the CNTs and the other components. Notably, during this stage, no balls were utilized to prevent any impact on the length of the CNTs that could arise from breakage. Instead, it was anticipated that the presence of spherical butadiene SAN would serve a comparable purpose as the balls, with minimal or no adverse effect on the CNT length. Following this, to eliminate any absorbed moisture, the blends were maintained in the oven at 85 $^{\circ}\text{C}$ for an additional 2 hours.

Subsequent to this, acetone (with a purity of 99.8%, sourced from Dr Mojallali Industrial Chemical Complex Co.) was added to each of the ABS/CNTs mixtures in a ratio of 0.1 g/ml . These mixtures were allowed to remain at room temperature for a span of 2 hours until complete dissolution occurred. This process led to the formation of a relatively uniform suspension in which agglomerates of carbon nanotubes were dispersed within a polymer solution. The dispersion was achieved utilizing the EMDT process, with parameters specified

in reference [24]. The resultant solutions were then cautiously introduced drop by drop into an ethanol medium (with a concentration of 96%, supplied by Dr Mojallali Industrial Chemical Complex Co.). This step induced the coagulation of nanocomposite granules [25]. Then, the granules were gathered, followed by multiple washings with distilled water. Following this, they were subjected to humidification within an oven set at a temperature of 80°C for a duration of 24 hours.

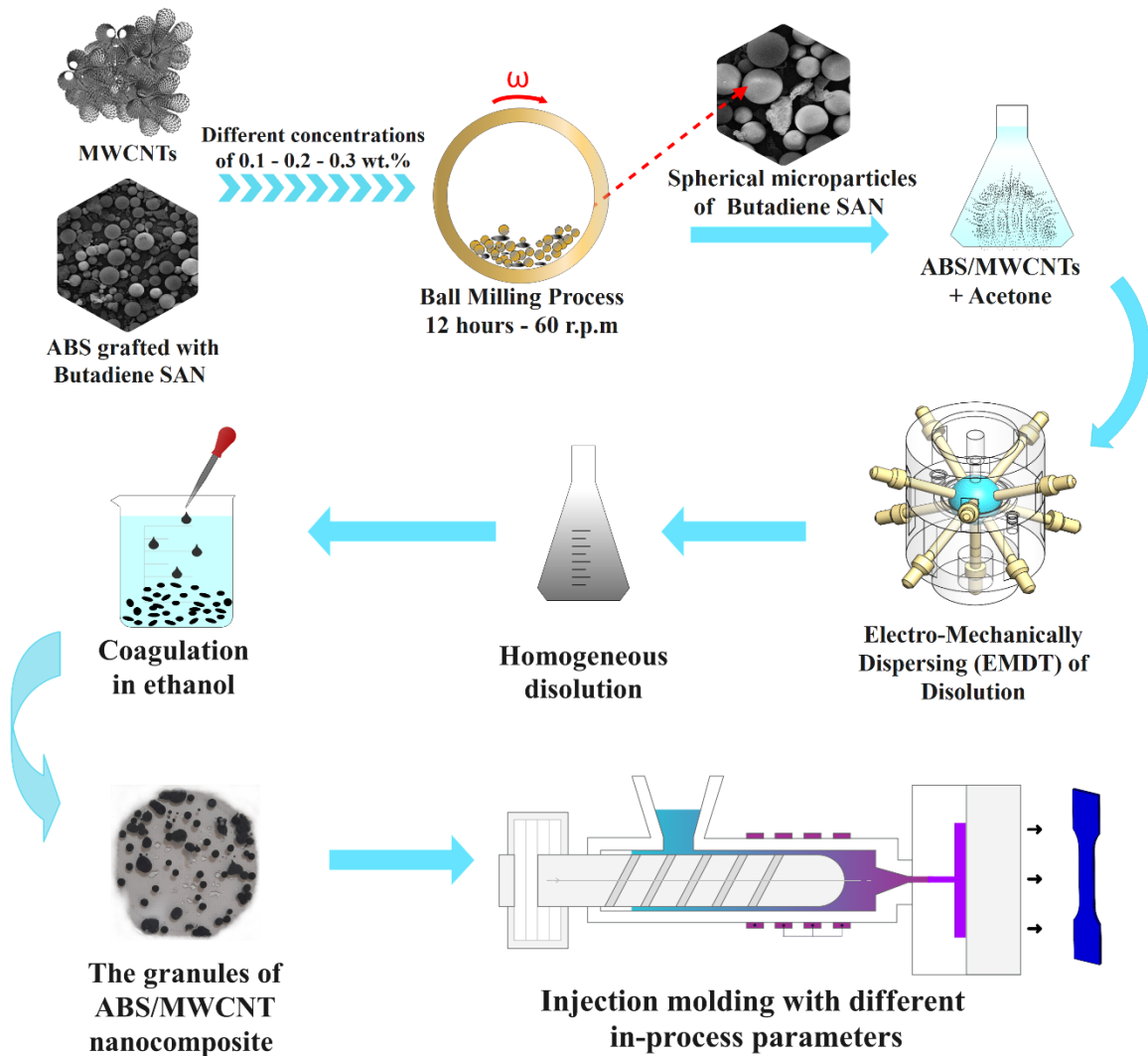


Fig. 1. General schematic of the followed process in this research to produce the samples

The samples were produced by Imen machine-Paya injection molding machine. In this step, injection temperature and holding pressure were considered as variable factors, while other parameters, including loading pressure 90 bar, cooling time 15 s, injection time 8 s, injection pressure 40 bar, injection speed 54.3 mm/s and mold temperature 70 °C were kept constant.

2.3. Design of Experiments

The experiments were designed using the full factorial method, wherein CNTs concentration, injection temperature, and holding pressure were considered as the variable factors. The experimental layout and the results of each experiment run are presented in **Table S2**.

2.4. Characterizations

The morphology of the powder and the injection-molded samples was analyzed using the OXFORD Leo 440i scanning electron microscope (SEM) and the TESCAN-MIRA3 field emission electron microscope (FE-SEM), respectively. To investigate the samples by FE-SEM, the nanocomposite granules produced with the EMDT method were frozen using liquid nitrogen and subsequently fractured. For further examination of agglomeration formation at higher CNT concentrations, the same approach as described in Ref [19] was followed, using an Olympus BX61 optical microscope (Olympus Corporation, Japan) equipped with an Olympus DP80 camera. To prepare the thin films, the nanocomposites were dissolved in acetone and then dripped onto a lamel. Additionally, to investigate the crystallinity and structure of the nanocomposites, X-ray diffraction (XRD) analysis was performed using a Tongda TD-3700 instrument.

The thermal properties of the ABS/MWCNT nanocomposite were determined through a differential scanning calorimetry (DSC) machine (PerkinElmer Thermal Analysis, DSC 8000) with a constant temperature change rate of ± 10 °C/min under a nitrogen flow at a rate of 20 ml/min, covering a temperature range from 40 to 270 °C. DSC thermograms were analyzed to assess the impact of MWCNT on the thermal and mechanical properties of ABS nanocomposites. Thermal gravimetric analysis (TGA) of the samples was conducted to determine their degradation temperatures. The analysis was performed using a Mettler

Toledo TGA/DSC 3+ instrument (Switzerland) at a heating rate of 10°C/min under a nitrogen (N₂) atmosphere, over a temperature range of 50°C to 750°C

Additionally, Raman analysis was conducted on the injected samples using a Jobin Yvin S-3000 device, featuring a resolution of 2 cm⁻¹ and laser characteristics with a wavelength of 514.5 nm, an effective diameter of 3 μm, and a radiation power of 1 mW. This analysis was carried out in both injection and perpendicular to flow directions. To determine the coefficient of thermal conductivity, a cylinder with a diameter of 22.58 mm was cut from the injected samples using a CO₂ laser cutting process. The measurement was carried out using a device specifically designed and fabricated for this purpose, following the ASTM D5470 standard and reference [26].

The tensile strength of the samples was measured according to the ASTM D638 standard. The measurement was repeated three times, utilizing an extensometer to enhance the precision of the tests. The microhardness of the samples was also measured using a Zwick-ZhV10 device at least ten different points on three samples, according to the ASTM E384 standard. Impact strength was determined by employing a Santam-SIT-50j machine, considering the Charpy method and conducting three repetitions based on the ASTM D6110 standard.

3. Result and discussion

3.1. Morphology

Fig. 2 displays scanning electron microscope (SEM) micrographs of pure ABS powder. The presence of PB spheres and SAN grafts is distinctly evident in the image. As initially anticipated, these spherical components have the potential to act like light-balls in the small-scale ball milling process, effectively reducing the entanglement and agglomeration of CNTs [12].

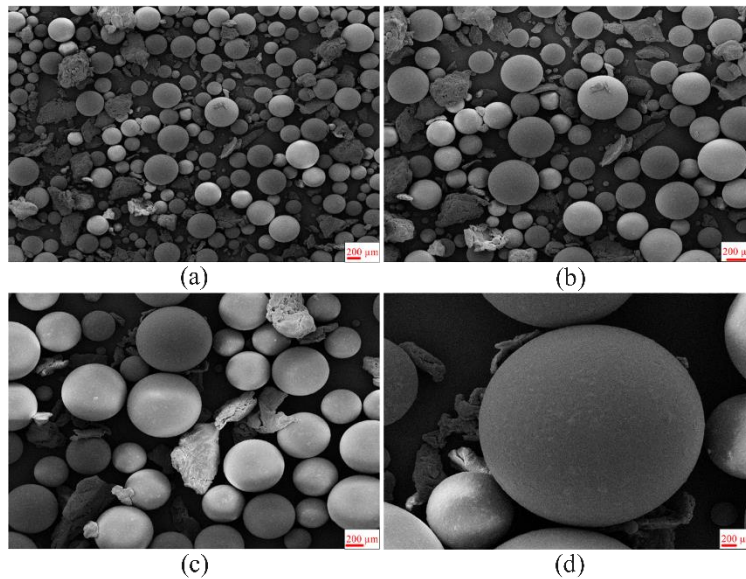


Fig. 2. :The SEM micrographs of ABS powder at different magnifications (a) 20 (b) 30 (c) 50 and (d) 70 X.

Real images are presented in the Supplementary Information section, **Figure S2**, showcasing the state of ABS/MWCTs before and after light ball milling. These images illustrate that, as expected, the dimensions of the agglomerations have significantly reduced after this process. **Fig. 3** displays FE-SEM micrographs of nanocomposites prepared using the EMDT method at different concentrations. It can be observed that at a concentration of 0.1%, there are no significant agglomerates. However, at a concentration of 0.2 wt.%, only limited agglomerations were observed, and at a concentration of 0.3 wt.%, numerous agglomerations with large dimensions were noticed. This indicates that during the EMDT process at high concentrations, the majority of agglomerations were attracted to the poles and remained intact [24]. This limitation is associated with melt mixing methods. When the concentration increases significantly, it becomes challenging to separate and break down the primary agglomerations into individual CNTs [27]. Optical microscope images showing agglomerations at 0.3 wt.% concentration are presented in the Supplementary Information section, **Figure S3**.

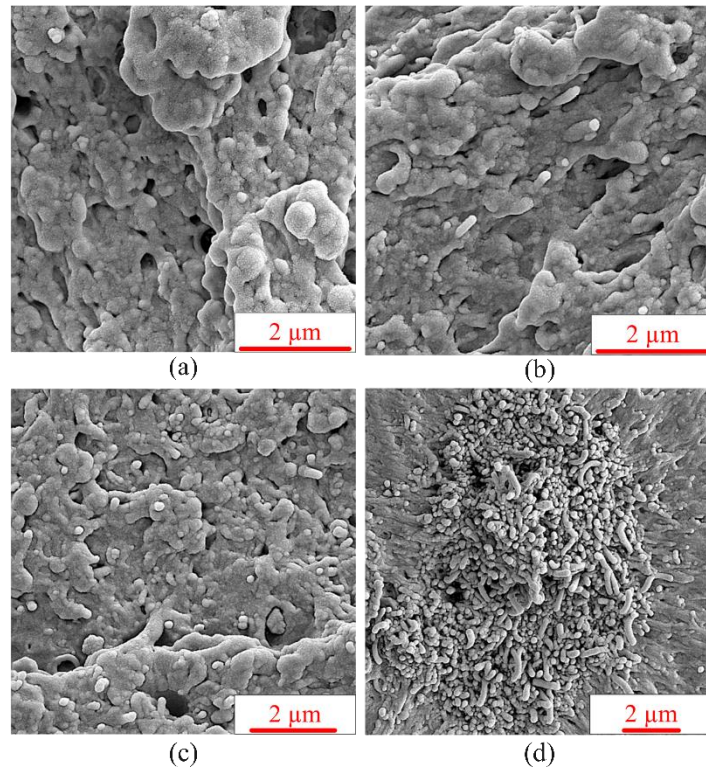


Fig. 3. FE-SEM microscopies of ABS/CNTs :nanocomposites prepared by EMDT at different concentration .%.a) 0, b) 0.1, c) 0.2 and d) 0.3 wt

To further investigate the structural characteristics of the nanocomposites XRD analysis were performed and the obtained patterns of MWCNT, pure ABS, and 0.2 wt.% ABS/MWCNT nanocomposite are presented in **Fig. 4**. In curve (a), the sharp peak at 26.01° corresponds to the (002) plane of graphitic carbon, confirming the presence of intact and crystalline MWCNT structures [28]. This peak is characteristic of the interlayer spacing within the MWCNTs and indicates their well-ordered graphitic nature. In curve (b), the broad peak observed between 10° and 30° , along with a sharper feature at 19.14° , is characteristic of the predominantly amorphous nature of ABS. The broad peak reflects the disordered arrangement of polymer chains, while the sharper peak at 19.14° indicates localized ordering or short-range crystallinity within the ABS structure [29]. This observation is supported by DSC results, which revealed a melting point for pure ABS, confirming the presence of a low degree of crystallinity.

In curve (c), the peak at 25.33° is attributed to the presence of MWCNTs in the nanocomposite. The slight shift from 26.01° in the pure MWCNT pattern may result from interactions between the MWCNTs and the ABS polymer matrix [29]. Additionally, the peaks at 37.70° , 47.98° , 53.79° , and 55.02° suggest the formation of more ordered crystalline regions in the composite. These peaks likely arise from the influence of MWCNTs, which act as nucleating agents for polymer crystallization, facilitating the alignment and ordering of polymer chains near the MWCNT surfaces.

The increased intensity and appearance of these peaks in the nanocomposite compared to pure ABS indicate changes in the crystallinity of the polymer matrix. The incorporation of MWCNTs enhances the degree of crystallinity by providing surfaces for heterogeneous nucleation and promoting the formation of ordered polymer domains. This structural modification reflects the strong interaction between the MWCNTs and the ABS matrix, which alters the overall crystal structure of the polymer.

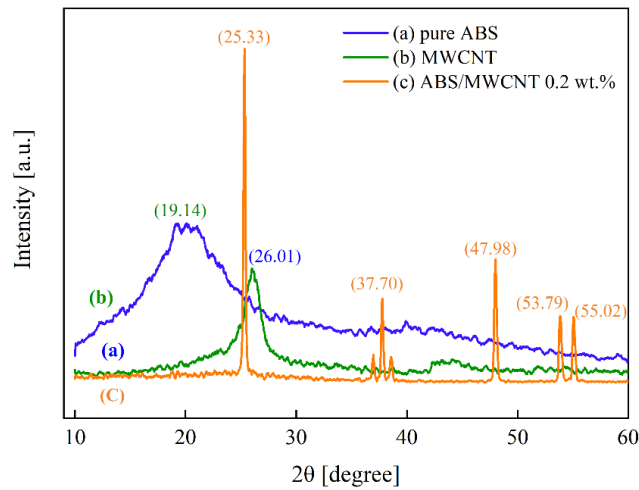


Fig. 4. XRD patterns of pure ABS, MWCNT, and 0.2 wt.% ABS/MWCNT nanocomposite samples.

3.2. Differential Scanning Calorimetry (DSC) and Thermal Gravimetric Analysis (TGA)

The DSC thermograms presented in **Fig. 5** were analyzed to investigate the influence of MWCNT on the thermal and mechanical properties of ABS nanocomposites. The

thermogram clearly demonstrates the impact of incorporating MWCNTs as a filler on the thermal properties of the ABS matrix. An evident small peak in the baseline is observed at approximately 105 °C, indicating the glass transition temperature (T_g) of pure ABS. This T_g is associated with the softening of the SAN copolymer phase within ABS [30]. The peaks specified within the range of 200-225 °C correspond to the melting temperature (T_m) of the composites [31, 32].

Fig. 5 clearly indicates that the CNTs led to an increase in the value of T_m . The main reason for this effect is the increase in the attractive force between polymer chains, resulting from the surface interaction between the polymer and CNTs. This trend is also observed in the case of T_g . It appears that CNTs acted as nucleating agents, leading to an elevation in the melting temperature of the polymer matrix [32]. Furthermore, the pronounced affinity of CNTs to interact with the polymer matrix hinders the mobility of polymer chains, leading to an increase in T_g [31].

Additionally, the DSC findings were utilized to assess the dispersion and distribution state of CNTs. If the degree of dispersion is high, it leads to an increase in the attractive force between nanoparticles and the polymer matrix. Consequently, the melting enthalpy rises, requiring more energy to break the bonds between polymer chains. However, the absence of dispersion leads to the formation of spatial obstacles within the polymer chain and among nanoparticles. This hinders rotation around the polymer chain link, resulting in a reduced demand for energy to facilitate heat transfer. Thus, there is a decrease in enthalpy [33].

The data obtained from DSC have also been summarized in **Table S3**. The trend of enthalpy increase can be observed from 0 to 0.2 wt.% as shown in **Table S3**. However, at 0.3 wt.%, a notable decrease in its value is evident. At this concentration level, improper dispersion and the presence of large agglomerations cause a slight change in the total heat of reaction. Based on the results obtained from this analysis, EMDT has successfully dispersed and separated nanotubes up to the concentration of 0.2 wt.%

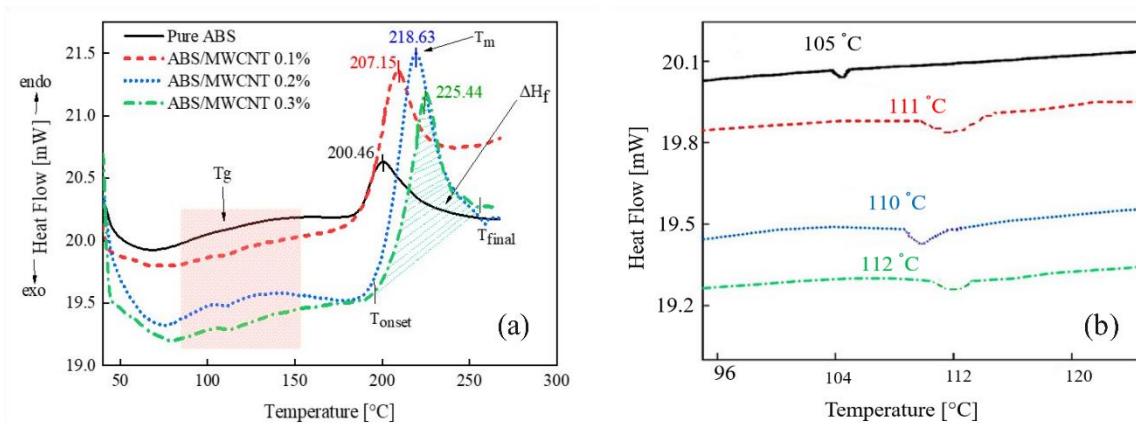


Fig. 5. DSC analysis of different nanocomposites prepared by EMDT: (a) thermograms and (b) zoom on T_g points

The TGA results are shown in **Fig. 6**, with additional details presented in **Table S4**. The data reveal that the onset of thermal decomposition (T_{onset}) for pure ABS occurs at 360 °C, which is earlier compared to the ABS/MWCNT nanocomposites. The T_{onset} for the nanocomposites begins at around 362 °C for 0.1 wt.% MWCNT, and increases to 378 °C, 382 °C for the 0.2 wt.% and 0.3 wt.% MWCNT composites, respectively. This indicates that the addition of MWCNTs delays the onset of thermal decomposition, suggesting enhanced thermal stability [29].

The maximum degradation temperature ($T_{d,max}$) for the pure ABS is 456 °C, whereas the nanocomposites exhibit slightly higher $T_{d,max}$ values (470 °C for 0.1 wt.%, 463 °C for 0.2 wt.%, and 467 °C for 0.3 wt.%). This indicates that the presence of MWCNTs further improves the thermal stability of the composites.

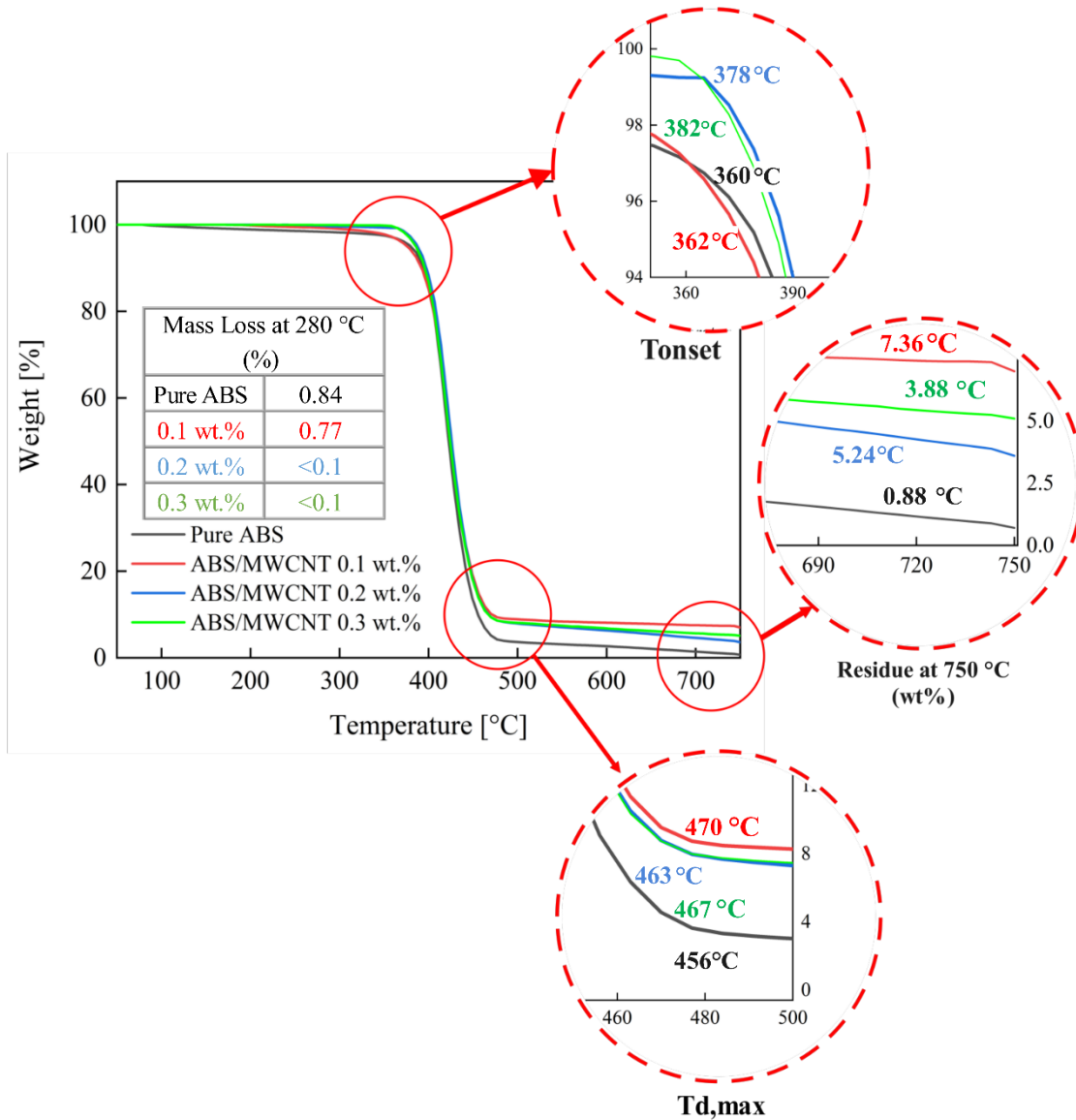


Fig. 6. TGA graphs of pure ABS and ABS/MWCNT nanocomposites with different MWCNT.

3.3. Raman analysis

Raman spectroscopy is widely used to assess the quality of carbon nanotubes. In the case of injection-molded samples, conducting Raman spectroscopy in two directions, along the flow and perpendicular to it, can determine the level of alignment of CNTs [34]. **Fig. 7** depicts the Raman spectrum of nanocomposite samples with a concentration of 0.2% under various injection conditions. In all spectra, there is a peak at 1002 cm^{-1} , corresponding to pure ABS and indicating the vibrational response of the aromatic ring in the styrene part of ABS. The characteristic peaks of MWCNTs appear around 1360 and 1600 cm^{-1} , known as the D and G

bands, respectively. The addition of nanotubes to the matrix significantly reduces the peak intensity of pure ABS [24]. The D band is related to vibrations caused by structural defects and is considered the most sensitive peak in Raman analysis for determining the orientation of carbon nanotubes [24]. On the other hand, the G band is related to the in-plane vibration of the carbon lattice with sp^2 hybridization and is less sensitive to orientation [23].

The peak intensity ratio (I_D/I_G) is used as a criterion for assessing the quality of carbon nanotubes. An increase in this ratio indicates the presence of nanotubes with high structural defects or the presence of amorphous carbon in the sample [24]. Additionally, the intensity ratios $D_{||}/D_{\perp}$ and $G_{||}/G_{\perp}$ are used to assess the degree of orientation of carbon nanotubes. Considering that the major characteristics of nanocomposites containing nanotubes, such as mechanical strength, thermal, and electrical conductivity, are significantly influenced by the alignment of nanotubes, determining their alignment becomes of utmost importance [35, 36]. **Fig. 7a** depicts the Raman spectra of both raw CNTs and ABS/CNTs powder after light ball milling. In the case of raw CNTs, the ratio remains 0.98 even after light ball milling, indicating that the application of light ball milling did not have any impact on the structure of the CNTs, even though their size was reduced [34].

The observed slight changes in the ABS peak intensity suggest that there is an interaction occurring between MWCNT and ABS [35]. The interaction between the components results in an enhancement of the nanocomposite sample's mechanical properties. The displacement pattern obtained from the Raman peak corresponds well with the mechanical data obtained. **Table 1** provides a concise classification of the peak intensities' ratios. To examine the structural changes in MWCNTs, researchers utilize the ratio $(D/G)_{||}/(D/G)_{\perp}$ [35]. **Table 1** reveals that the intensity ratio $(D/G)_{||}/(D/G)_{\perp}$ for samples obtained through injection molding is approximately 1, with minimal variations under different injection conditions. This finding shows that the carbon nanotube structure remains relatively undamaged despite the changes in injection parameters [35].

The analysis of **Table 1** reveals an interesting pattern in samples A₁, A₃, and A₅. Specifically, when the holding pressure is raised, there is a notable decrease in the intensity ratio of peaks $(D/G)_{||}/(D/G)_{\perp}$. This observation points toward a reduced orientation of carbon nanotubes in these particular samples under higher holding pressure conditions. In contrast, when

analyzing samples A₂, A₄, and A₆, it becomes evident that a higher holding pressure leads to a notable improvement in the orientation of carbon nanotubes. However, it is noteworthy that at low temperatures, increasing the pressure does not yield the desired orientation, as suggested by the available data [36]. The reason for this phenomenon can be attributed to the exposure of the polymer in a viscous state to shearing and stretching forces during the injection molding process, as indicated in previous research [33]. These forces have a strong impact on the CNTs network and result in the formation of a core-shell structure [35]. Consequently, the alignment of CNTs becomes closer to the surface of the piece. As the holding pressure increases, the nanotubes exhibit more curvature and form worm-like structures instead of remaining straight [37]. Moreover, in scenarios where the medium is viscous, increasing the pressure leads to structural damage to CNTs, which is supported by the D/G ratio presented in **Table 1** of this analysis. Therefore, by elevating the injection temperature and reducing the holding pressure, a significant number of existing CNTs can be partially aligned.

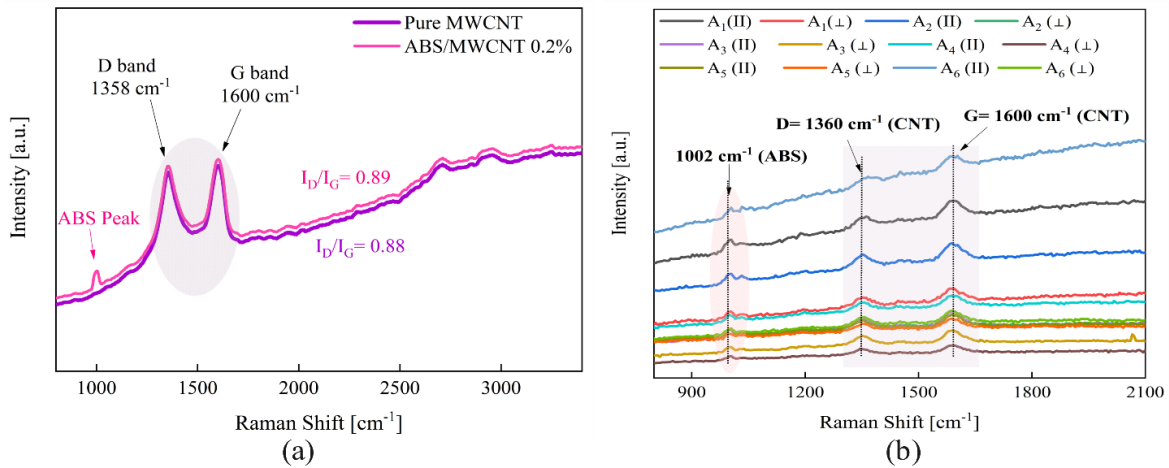


Fig. 7. Raman spectra of ABS/MWCNT nanocomposites at the concentration of (0.2 wt.%). (a) before injection molding, and (b) after injection molding with different in-process factors: sample A₁ (T= 210 °C, P= 50 bar), sample A₂ (T= 220 °C, P= 50 bar), sample A₃ (T= 210 °C, P=60 bar), sample A₄ (T= 220 °C, P= 60 bar), sample A₅ (T= 210 °C, P= 70 bar), sample A₆ (T= 220 °C, P= 70 bar), || = Parallel, ⊥ = Perpendicular.

Table 1. Raman intensity ratios parallel/perpendicular for the injection-molded samples of ABS/MWCNT 0.2 wt.%.

Sample (0.2 wt.%)	Temperature [°C]	Pressure [bar]	$\frac{D_{\parallel}}{D_{\perp}}$	$\frac{G_{\parallel}}{G_{\perp}}$	$\frac{D_{\perp}}{D_{\parallel}}$	$(\frac{I_D}{I_G})_{\parallel}$	$(\frac{I_D}{I_G})_{\perp}$	$\frac{(\frac{I_D}{I_G})_{\parallel}}{(\frac{I_D}{I_G})_{\perp}}$
A ₁	210	50	1.78	1.82	0.56	0.925	0.942	0.981
A ₂	220	50	1.79	1.81	0.55	0.926	0.934	0.991
A ₃	210	60	1.29	1.26	0.77	0.948	0.931	1.01
A ₄	220	60	1.91	1.92	0.52	0.932	0.940	0.991
A ₅	210	70	1.03	1.04	0.97	0.926	0.938	0.987
A ₆	220	70	2.69	2.82	0.37	0.903	0.953	0.947

I_D/I_G (Pure MWCNT) = 0.88
 I_D/I_G (Powder ABS/MWCNT 0.2%) = 0.89

The strain-stress curves of the samples obtained from the tensile analysis are illustrated in **Fig. 8a**. These curves clearly demonstrate the significant impact of injection and sample preparation conditions on crucial mechanical properties. To provide a more comprehensive analysis, the numerical values corresponding to these specifications are presented in **Fig. 8b**, **8c**, and **8d**. The incorporation of carbon nanotubes up to 0.2 wt.% results in an increase in the modulus of elasticity, ultimate tensile strength, and yield stress. However, when the weight percentage of nanotubes exceeds 0.3%, a decline in overall mechanical strength becomes evident. These results validate the microscopic findings. As previously mentioned, EMDT functions effectively at low concentrations (up to 0.2%). However, when dealing with higher concentrations, this process encounters challenges in adequately distributing and isolating the agglomerates [12].

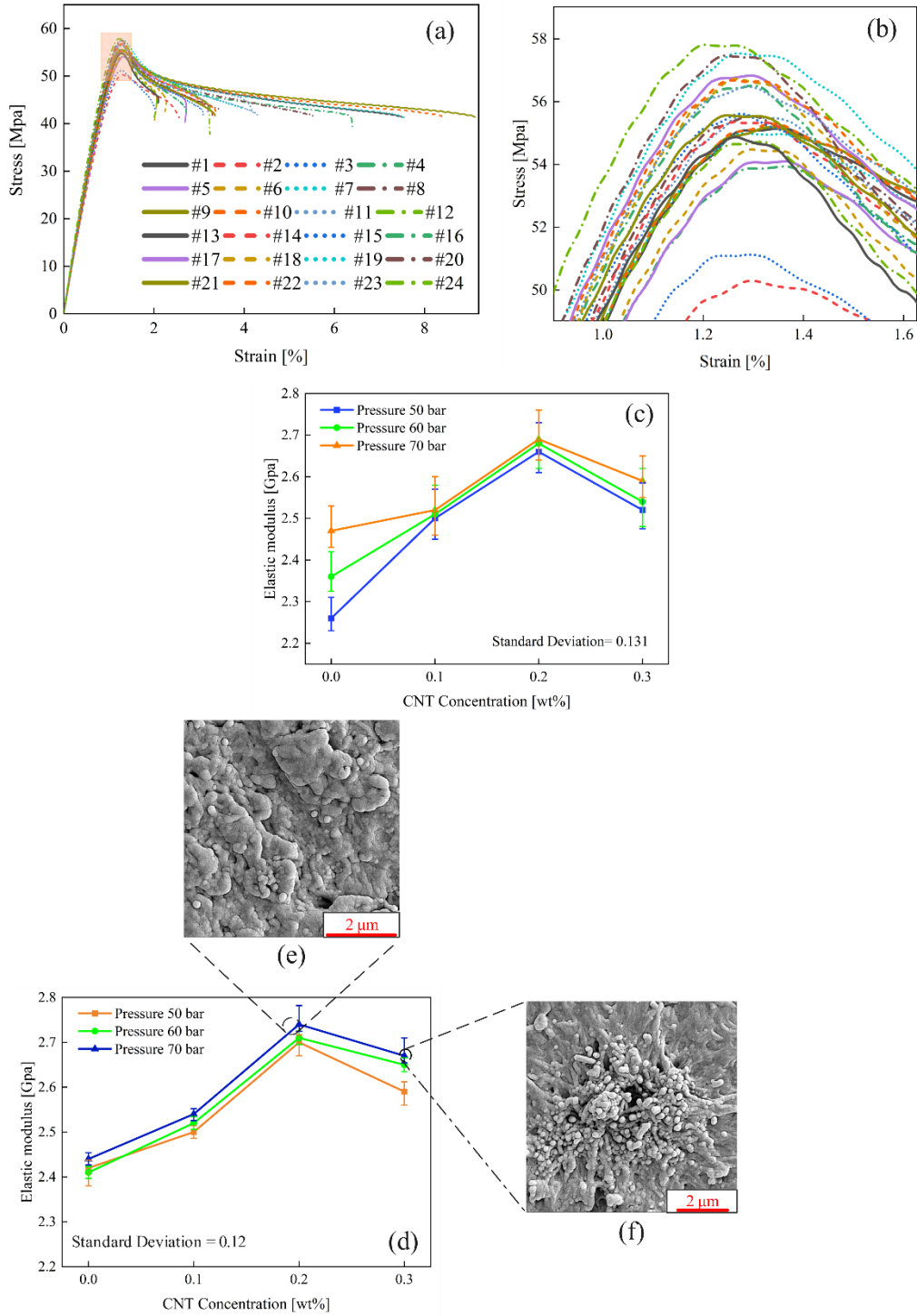


Fig. 8: Mechanical properties of injection-molded samples with varied injection temperature and holding pressure. (a) Strain-stress curve of the samples (Sample production conditions detailed in **Table 2**), (b) Zoomed-in Strain-Stress plot, (c) Elastic modulus for T=210 °C, (d) Elastic modulus for T=220 °C, (e) and (f) Corresponding FE-SEM micrographs of nanocomposites.

Fig. 9 demonstrates the yield and ultimate strength of samples. The presence of remaining large agglomerates at higher concentrations behaves like impurities within the nanocomposite matrix, contributing to a decline in the material's mechanical strength [38, 39]. At low concentrations, the nanotubes exhibit a high degree of dispersion, creating a stable and beneficial interaction with the matrix material [39]. This, in turn, facilitates a substantial transfer of the applied load to the nanotubes, enhancing the overall mechanical performance [40]. It is widely acknowledged in scientific reports that there is a saturation limit to which carbon nanotubes can be added to the base polymer to reinforce its strength. This limitation applies not only to EMDT but also to other methods [41].

The data from **Table. 2** clearly indicates that raising the injection temperature and holding pressure has a positive impact on the enhancement of E (elastic modulus), Y (yield stress), and σ_{uts} (maximum tensile strength). It has been proven that there is an increase in the alignment of CNTs along the injection direction by Raman analysis [42, 43]. This alignment improvement is a significant factor that positively impacts the tensile properties of the material [13]. However, it is worth noting that there are reports indicating that an increase in the injection temperature not only promotes orientation and dispersion but also negatively influences mechanical properties, such as yield stress [44].

Comparing the obtained results with existing references shows that the utilization of EMDT allows for achieving superior mechanical strength with a small amount of nanotubes [40]. Higher mechanical strength can be attributed to two key advantages of EMDT: I) it effectively protects the length of carbon nanotubes and facilitates efficient spreading and dispersion of the nanotubes [24]. II) during the EMDT process, a significant amount of electric charge is accumulated on the carbon nanotubes [24], which is likely to facilitate the formation of a strong layer between the matrix and the nanotubes by promoting a chemical bond [45]. This enhancement leads to an increase in the strength of the nanocomposites.

Numerical comparison of the results with other studies indicates that the utilization of EMDT has led to a noteworthy enhancement in the modulus of elasticity by merely adding 0.2 wt.% of carbon nanotubes, resulting in an 18% and 14% increase, respectively. However, for achieving similar results using the melt mixing method, at least 2 wt.% of carbon nanotubes are necessary. In CNT-based nanocomposites, enhancing mechanical strength heavily

depends on the interfacial bonding between the matrix and CNTs, as this interface facilitates load transfer to the CNTs, which are stronger than the polymeric matrix, resulting in remarkable mechanical strength [46]. EMDT plays a pivotal role in forming interfacial bonding for two main reasons: 1) It provides higher CNT length after dispersion, leading to a more developed interfacial layer [47], and 2) it accumulates considerable charges (electrons) on the CNTs, which increases the polar nature of their surface [24]. ABS is a polar polymer with functional groups, such as nitrile groups, that can interact with the charged CNTs. The enhanced polar interactions promote stronger interfacial adhesion between the CNTs and the ABS matrix, facilitating better load transfer [48]. In addition to enhancing polar interactions, charging the surface of CNTs through EMDT can positively influence electrostatic attraction, promoting better dispersion and aligning functional groups for more efficient bonding. Consequently, these molecular-level improvements in interfacial bonding lead to significant mechanical property enhancements, such as increased tensile strength and modulus, as the load is more effectively transferred to the stronger CNTs [49].

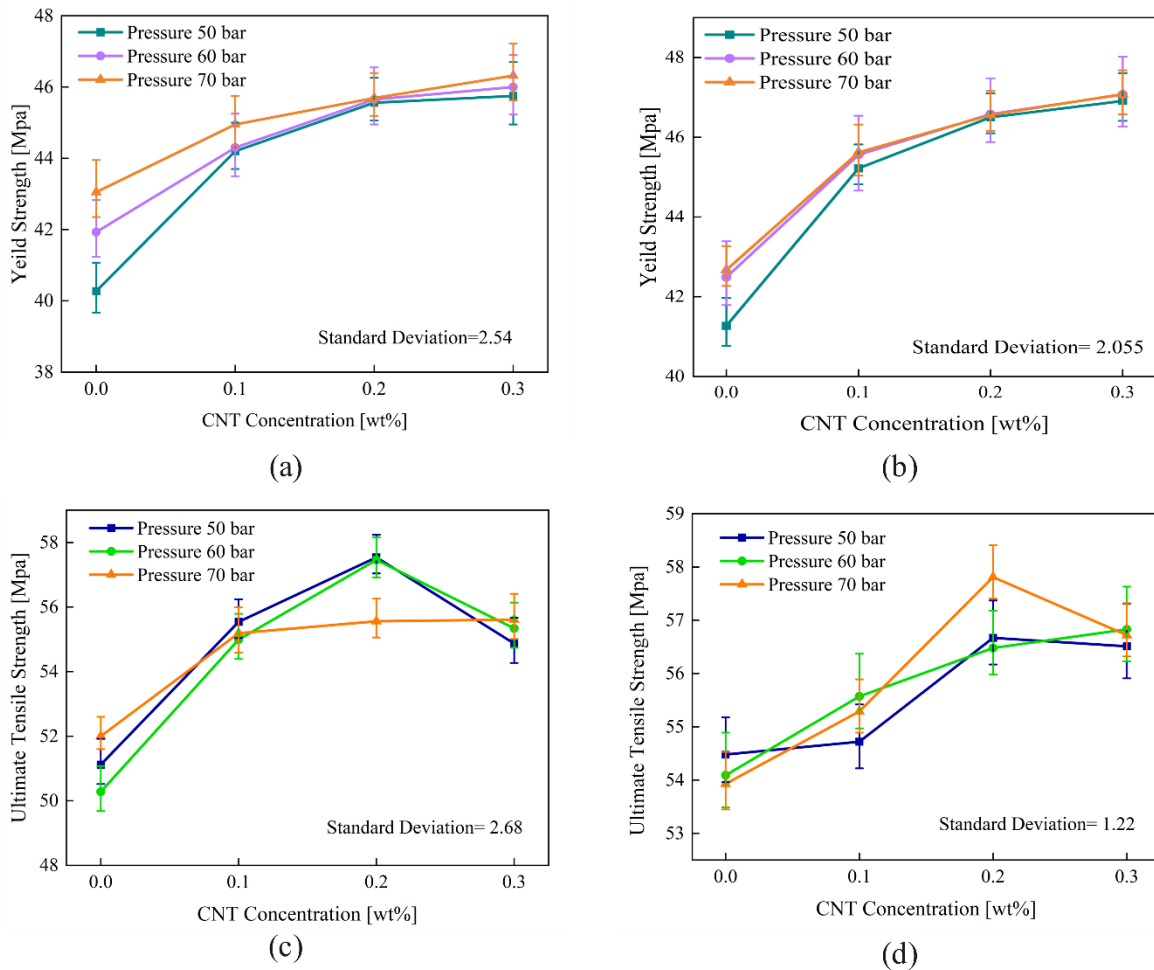


Fig. 9. Mechanical characteristics of the samples: yield strength for (a) T=210 °C, (b) T=220 °C, ultimate tensile strength for (c) T=210 °C and (d) T=220 °C.

As previously discussed, increasing the temperature helps in reducing CNT entanglement and promoting better alignment, thereby enhancing the strength of the nanocomposite. Both Young's modulus and ultimate tensile strength exhibit improvement up to a concentration of 0.2% and a subsequent decline at 0.3%, primarily due to agglomerate formation.

The primary factor contributing to this issue appears to be the limited interaction between the nanotubes and the matrix [24]. Without the formation of a strong interface layer to transfer the load to the nanotubes, a typical consequence is a reduction in strength [42]. The sample containing 0.2 wt.% CNTs, injected at 220 °C and subjected to a holding pressure of 70 bars, demonstrated the highest tensile strength. Despite Raman spectroscopy indicating a lower alignment degree under these conditions, the strength enhancement can be attributed to

smaller agglomerates, better distribution, and reduced CNT entanglement, which enhanced interfacial bonding. Thus, it appears that interfacial bonding plays a more prominent role than the alignment degree in determining the tensile strength.

3.4. Thermal Conductivity

Fig. 10 depicts the thermal conductivity coefficients of the samples. A comparison between **Fig. 10a** and **b** reveals that the thermal conductivity is greater for the samples injected at a temperature of 220 °C. This noticeable difference stems from the improved orientation of CNTs and the development of a conductive network at elevated temperatures [43, 45]. Increasing the CNT concentration up to 0.2% resulted in enhanced thermal conductivity in all instances, with no significant alteration observed upon further increasing it to 0.3 wt.%. Microscopic examinations unveiled that at this CNT concentration level, EMDT fails to completely disperse the nanotubes, leaving a substantial portion of agglomerations intact. Consequently, the process of compacting the CNT network, a pivotal factor in thermal conduction [50], halts because EMDT cannot further disperse the agglomerates and individualize the CNTs. Furthermore, 0.2 wt.% can be considered as a percolation threshold concentration for thermal conductivity as beyond this level the conductivity approximately remains constant.

The increase in thermal conductivity becomes evident as the holding pressure rises. Higher pressure plays a vital role in both compacting the CNT network and enhancing their alignment during the injection process [51], as confirmed by Raman findings. Despite other researchers using significantly higher concentrations for ABS/MWCNTs nanocomposites prepared via melt mixing and ultrasonication methods, the thermal conductivity remains significantly lower than the maximum achieved in this study (0.31 W/mK) [51]. This accomplishment demonstrates that the EMDT process can substantially enhance the properties even at low concentrations by preserving the pristine length of the nanotubes [24]. Hence, it can be summarized that higher CNTs' length provided by EMDT can improve the CNT-CNT network density and enhance thermal conductivity significantly.

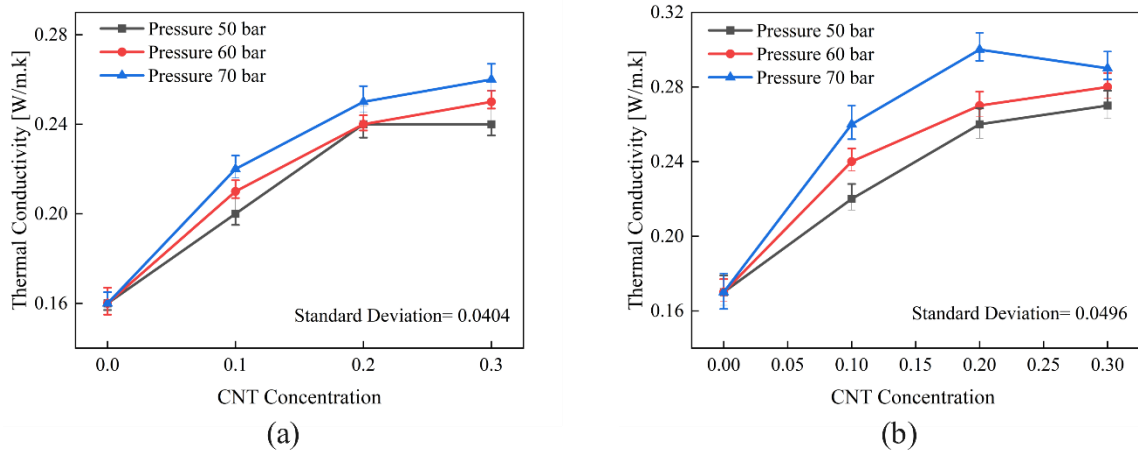


Fig. 10. Thermal conductivity of samples produced by different injection temperature and holding pressure: (a) T=210 °C, (b) T=220 °C.

Fig. 11 illustrates the impact strength of nanocomposites. A comparison between Fig. 10 a and b reveals that nanocomposites produced at a temperature of 220 °C exhibit slightly lower strength. At both temperatures and a concentration of 0.1, modifying the holding pressure led to a minor increase in impact strength. However, with an increase in concentration to 0.2% and 0.3 wt.%, this process induced certain changes and led to a decrease in strength. The results suggest that at higher concentrations, the impact of partial alignment through the injection flow is considerably weaker when contrasted with the CNTs network density [41, 50]. The rise in CNT concentration results in a reduction in impact strength and is also associated with a shift in fracture behavior from a soft to a brittle state [42].

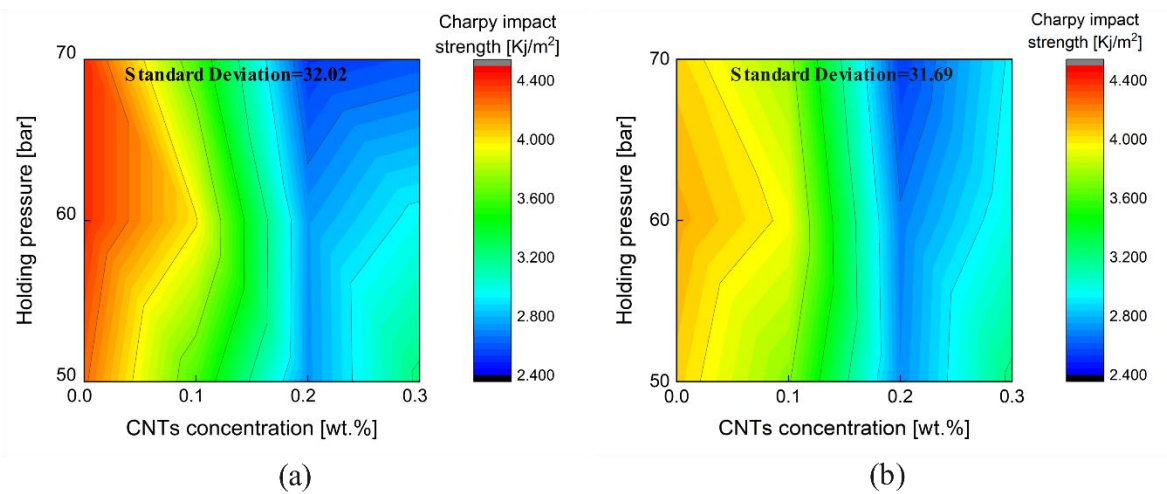


Fig. 11. Impact strength of samples produced by different injection temperature and holding pressure: (a) T=210 °C, (c) T=220 °C.

4. Conclusion

This research involved the preparation of ABS/MWCNTs nanocomposites using the EMDT method, examining its impact on reducing the required concentration of CNTs to achieve significant improvements in thermal and mechanical properties. The findings indicate:

The EMDT method effectively disperses CNTs up to a concentration of 0.2 wt.%. However, beyond this concentration, large agglomerates of CNTs remain prevalent in the matrix. This technique bolsters tensile strength with the incorporation of a mere 0.2 wt.% of CNTs, resulting in a tensile strength value of approximately 2.74 GPa. In contrast, conventional methods demand 10 times the amount of CNTs to attain a similar level of mechanical reinforcement for ABS. This underscores the efficacy of EMDT in reducing the necessary CNT concentration while simultaneously preserving their length and forming a robust interface layer due to the electrical charges on CNTs. Furthermore, it positively influences thermal conductivity by maintaining the nanotubes' length. The inclusion of only 0.2 wt.% of CNTs leads to a significant 48.4% increase in conductivity, achieving a value of 0.31 W/mK.

Another noteworthy discovery is the decline in impact strength of the samples attributed to the incorporation of CNTs, resulting in a shift from a soft to a brittle fracture behavior. Adjusting the injection temperature to 220 °C and maintaining the holding pressure at 70 bar during the injection molding process enhance the alignment of CNTs and reduce entanglement, leading to higher both thermal and mechanical properties.

Declaration of Competing Interest

The authors declare that they have no known competing financial interests or personal relationships that could have appeared to influence the work reported in this paper.

References

[1] Shin WH, Kim S, Kim SY. Theoretical modeling for piezoresistive behavior of aligned carbon nanotube/polymer nanocomposites accounting for evolution of agglomerates morphology. *Mater. Today Commun.* 2023; 34: 104931.

<https://doi.org/10.1016/j.mtcomm.2022.104931>

[2] Sheng Y, Li C, Wang J, Xia X, Wen GJ, Su Y. Multiscale modeling of thermal conductivity of hierarchical CNT-polymer nanocomposite system with progressive agglomeration. *Carbon.* 2023; 201: 785-795.

<https://doi.org/10.1016/j.carbon.2022.09.057>

[3] Ogbonna VE, Popoola API, Popoola OM. A review on recent advances on the mechanical and conductivity properties of epoxy nanocomposites for industrial applications. *Polym. Bull.* 2023; 80: 3449-3487.

<https://doi.org/10.1007/s00289-022-04249-4>

[4] Sahu SK, Rama Sreekanth PS. Mechanical, thermal and rheological properties of thermoplastic polymer nanocomposite reinforced with nanodiamond, carbon nanotube and graphite nanoplatelets. *Adv. Mater. Process. Technol.* 2022; 8: 2086-2096.

<https://doi.org/10.1080/2374068X.2022.2034309>

[5] Miyashiro D, Hamano R, Umemura K. A review of applications using mixed materials of cellulose, nanocellulose and carbon nanotubes. *Nanomater.* 2020; 10: 186.

<https://doi.org/10.3390/nano10020186>

[6] Yang Z, Tian J, Yin Z, Cui C, Qian W, Wei F. Carbon nanotube-and graphene-based nanomaterials and applications in high-voltage supercapacitor: A review. *Carbon.* 2019; 141: 467-480.

<https://doi.org/10.1016/j.carbon.2018.10.010>

[7] Lavagna L, Nisticò R, Musso S, Pavese M. Functionalization as a way to enhance dispersion of carbon nanotubes in matrices: A review. *Mater. Today Chem.* 2021; 20: 100477.

<https://doi.org/10.1016/j.mtchem.2021.100477>

[8] Strozzi M, Smirnov VV, Pellicano F, Kovaleva M. Nonlocal anisotropic elastic shell model for vibrations of double-walled carbon nanotubes under nonlinear van der Waals interaction forces. *Int. J. Non Linear. Mech.* 2022; 1461: 104172.

<https://doi.org/10.1016/j.ijnonlinmec.2022.104172>

[9] Hajian A, Lindstrom SB, Pettersson T, Hamed MM, Wågberg L. Understanding the dispersive action of nanocellulose for carbon nanomaterials. *Nano Lett.* 2017; 17: 1439-1447.

<https://doi.org/10.1021/acs.nanolett.6b04405>

[10] Rennhofer H, Zanghellini B. Dispersion state and damage of carbon nanotubes and carbon nanofibers by ultrasonic dispersion: a review. *Nanomater.* 2021; 11: 1469.

<https://doi.org/10.3390/nano11061469>

[11] Gao X, Isayev AI, Zhang X. Continuous film casting of polycarbonate/single-walled carbon nanotubes composites with ultrasound-assisted twin-screw extruder: Effect of screw configuration. *J. Appl. Polym. Sci.* 2022; 139: 53172.

<https://doi.org/10.1002/app.53172>

[12] Mousavi SR, Estaji S, Kiaei H, Mansourian-Tabaei M, Nouranian S, Jafari SH, Khonakdar HA. A review of electrical and thermal conductivities of epoxy resin systems reinforced with carbon nanotubes and graphene-based nanoparticles. *Polym. Test.* 2022; 107645.

<https://doi.org/10.1016/j.polymertesting.2022.107645>

- [13] Navidfar A, Azdast T, Karimzad Ghavidel A. Influence of processing condition and carbon nanotube on mechanical properties of injection molded multi-walled carbon nanotube/poly (methyl methacrylate) nanocomposites. *J. Appl. Polym. Sci.* 2016; 133: 43738. <https://doi.org/10.1002/app.43738>
- [14] Zhu P, Chow WS, Rusli A. Electrical conductivity and tensile properties of carbon nanotube reinforced styrene-ethylene-butylene-styrene thermoplastic elastomer nanocomposites. *J. Thermoplast. Compos. Mater.* 2023; 36: 3552-65. <https://doi.org/10.1177/08927057221131228>
- [15] Calderón-Villajos R, López AJ, Peponi L, Manzano-Santamaría J, Ureña A. 3D-printed self-healing composite polymer reinforced with carbon nanotubes. *Mater. Lett.* 2019; 249: 91-4. <https://doi.org/10.1016/j.matlet.2019.04.069>
- [16] Wang Z, Fan X, Wang K, Deng H, Chen F, Fu Q. Fabrication of polypropylene/carbon nanotubes composites via a sequential process of (rotating solid-state mixing)-plus-(melt extrusion). *Compos. Sci. Technol.* 2011; 71: 1397-403. <https://doi.org/10.1016/j.compscitech.2011.05.012>
- [17] McClory C, McNally T, Baxendale M, Pötschke P, Blau W, Ruether M. Electrical and rheological percolation of PMMA/MWCNT nanocomposites as a function of CNT geometry and functionality. *Eur. Polym. J.* 2010; 46: 854-68. <https://doi.org/10.1016/j.eurpolymj.2010.02.009>
- [18] Enqvist E, Ramanenka D, Marques PA, Gracio J, Emami N. The effect of ball milling time and rotational speed on ultra high molecular weight polyethylene reinforced with multiwalled carbon nanotubes. *Polym. Compos.* 2016; 37: 1128-1136. <https://doi.org/10.1002/pc.23275>

[19] Elbadawi NA, Ramadan AR, Esawi AM. Studying the effect of shortening carbon nanotubes via ball milling on cellulose acetate nanocomposite membranes for desalination applications. *Membranes*. 2022; 12: 474.

<https://doi.org/10.3390/membranes12050474>

[20] Pötschke P, Mothes F, Krause B, Voit B. Melt-mixed PP/MWCNT composites: influence of CNT incorporation strategy and matrix viscosity on filler dispersion and electrical resistivity. *Polymers*. 2019; 11: 189.

<https://doi.org/10.3390/polym11020189>

[21] Evgin T, Koca HD, Horny N, Turgut A, Tavman IH, Chirtoc M, Novak I. Effect of aspect ratio on thermal conductivity of high density polyethylene/multi-walled carbon nanotubes nanocomposites. *Compos. Part A Appl. Sci. Manuf.* 2016; 82: 208-213.

<https://doi.org/10.1016/j.compositesa.2015.12.013>

[22] Verma P, Saini P, Choudhary V. Choudhary, Designing of carbon nanotube/polymer composites using melt recirculation approach: Effect of aspect ratio on mechanical, electrical and EMI shielding response. *Mater. Des.* 2016; 88: 269-277.

<https://doi.org/10.1016/j.matdes.2015.08.156>

[23] Ghavidel AK, Zadshakoyan M, Arjmand M, Kiani G. A novel electro-mechanical technique for efficient dispersion of carbon nanotubes in liquid media. *Int. J. Mech. Sci.* 2021; 207: 106633.

<https://doi.org/10.1016/j.ijmecsci.2021.106633>

[24] Karimzad-Ghavidel A, Zadshakoyan M, Arjmand M. Mechanical analysis of aligned carbon nanotube bundles under electric field. *Int. J. Mech. Sci.* 2021; 196: 106289.

<https://doi.org/10.1016/j.ijmecsci.2021.106289>

- [25] Mohammadi A, Shojaei A, Khasraghi SS, Ghavidel AK. Synthesis of high-reinforcing-silica@ nanodiamond nanohybrids as efficient particles for enhancement of mechanical, thermal, and rolling resistance of styrene-butadiene rubber. *Polymer*. 2022; 255: 125122.
<https://doi.org/10.1016/j.polymer.2022.125122>
- [26] Watt MR, Gerhardt RA. Effect of processing on the properties and morphology of MWCNT-polymer networks. *Mater. Res. Express*. 2020; 7: 015075.
<https://doi.org/10.1088/2053-1591/ab67fd>
- [27] Rubel RI, Ali MH, Jafor MA, Alam MM. Carbon nanotubes agglomeration in reinforced composites: A review. *AIMS Mater. Sci*. 2019; 6: 756-780.
<https://doi.org/10.3934/matersci.2019.5.756>
- [28] Ullah Rather S. Preparation, characterization and hydrogen storage studies of carbon nanotubes and their composites: a review. *Int. J. Hydrog. Energy*. 2020; 45: 4653-4672.
<https://doi.org/10.1016/j.ijhydene.2019.12.055>
- [29] Mohammadsalih ZG, Abdulameer AF, Sadeq NS, Abbas LK, & Sapuan SM. Preparation, characterization, and properties of acrylonitrile butadiene styrene/multi walled carbon nanotubes nanocomposites. *J. Polym. Res*. 2024; 31: 203.
<https://doi.org/10.1007/s10965-024-04047-8>
- [30] Maiti S, Shrivastava NK, Khatua BB. Reduction of percolation threshold through double percolation in melt-blended polycarbonate/acrylonitrile butadiene styrene/multiwall carbon nanotubes elastomer nanocomposites. *Polym. Compos*. 2013; 34: 570-579.
<https://doi.org/10.1002/pc.22462>
- [31] Le TH, Le VS, Dang QK, Nguyen MT, Le TK, Bui NT. Microstructure evaluation and thermal–mechanical properties of abs matrix composite filament reinforced with multi-

walled carbon nanotubes by a single screw extruder for fdm 3d printing. *Appl. Sci.* 2021; 11: 8798.

<https://doi.org/10.3390/app11198798>

[32] Ujfalusi Z, Pentek A, Told R, Schiffer A, Nyitrai M, Maroti P. Detailed thermal characterization of acrylonitrile butadiene styrene and polylactic acid based carbon composites used in additive manufacturing. *Polymers.* 2020; 12: 2960.

<https://doi.org/10.3390/polym12122960>

[33] Kapoor S, Goyal M, Jindal P. Enhanced thermal, static, and dynamic mechanical properties of multi-walled carbon nanotubes-reinforced acrylonitrile butadiene styrene nanocomposite. *J. Thermoplast. Compos. Mater.* 2022; 35: 216-280.

<https://doi.org/10.1177/0892705719886012>

[34] Jindal P, Jyoti J, Kumar N. Mechanical characterization of ABS/MWCNT composites under static and dynamic loading conditions. *J. Mech. Eng. Sci.* 2016; 10: 2288-2299.

<https://doi.org/10.15282/jmes.10.3.2016.7.0213>

[35] Granada JE, Maron GK, Beatrice CA, Larocca NM, Moreira EC, Alano JH, deOliveira AD. Effect of carbon nanotubes functionalization on properties of their nanocomposites with polycarbonate/poly (acrylonitrile-butadiene-styrene) matrix. *J. Appl. Polym. Sci.* 2021; 138: 50471.

<https://doi.org/10.1002/app.50471>

[36] Gutierrez BJA, Dul S, Pegoretti A, Alvarez-Quintana J, Fambri L. Investigation of the effects of multi-wall and single-wall carbon nanotubes concentration on the properties of ABS nanocomposites. *Carbon.* 2021; 7: 33.

<https://doi.org/10.3390/c7020033>

[37] Wegrzyn M, Sahuquillo O, Benedito A, Gimenez E. Morphology, mechanical performance, and nanoindentation behavior of injection molded PC/ABS-MWCNT nanocomposites. *J. Appl. Polym. Sci.* 2015; 132: 1-8.

<https://doi.org/10.1002/app.42014>

[38] Dul S, Gutierrez BJA, Pegoretti A, Alvarez-Quintana J, Fambri L. 3D printing of ABS Nanocomposites. Comparison of processing and effects of multi-wall and single-wall carbon nanotubes on thermal, mechanical and electrical properties. *J. Mater. Sci. Technol.* 2022; 121: 52-66.

<https://doi.org/10.1016/j.jmst.2021.11.064>

[39] Wegrzyn M, Galindo B, Benedito A, Giménez E. Effect of Processing Method on Mechanical Properties of PC/ABS-MWCNT Nanocomposites. *Macromol. Symp.* 2012; 321: 161-165.

<https://doi.org/10.1002/masy.201251128>

[40] Jyoti J, Basu S, Singh BP, Dhakate SR. Superior mechanical and electrical properties of multiwall carbon nanotube reinforced acrylonitrile butadiene styrene high performance composites. *Compos. B: Eng.* 2015; 83: 58-65.

<https://doi.org/10.1016/j.compositesb.2015.08.055>

[41] Adhikary SK, Rudžionis Z, Rajapriya R. The effect of carbon nanotubes on the flowability, mechanical, microstructural and durability properties of cementitious composite: An overview. *Sustainabil.* 2020; 12: 8362.

<https://doi.org/10.3390/su12208362>

[42] Oseli A, Tomković T, Hatzikiriakos SG, Vesel A, Arzenšek M, Rojac T, Perše LS. Carbon nanotube network formation and configuration/morphology on reinforcing and conductive performance of polymer-based nanocomposites. *Compos. Sci. Technol.* 2023; 237: 110010.

<https://doi.org/10.1016/j.compscitech.2023.110010>

[43] Ghavidel AK, Lawrence J, Moradi M. Influence of the different nanostructures of acrylonitrile butadiene styrene/carbon nanotubes nanocomposites on laser cutting properties: Machining and chemical aspects. *Opt. Laser Technol.* 2023; 160: 108973.

<https://doi.org/10.1016/j.optlastec.2022.108973>

[44] Mahmoodi M, Lee YH, Mohamad A, Park SS. Effect of flow induced alignment on the thermal conductivity of injection molded carbon nanotube-filled polystyrene nanocomposites. *Polym. Eng. Sci.* 2015; 55: 753-762.

<https://doi.org/10.1002/pen.23942>

[45] Doagou-Rad S, Islam A, Søndergaard Jensen J. Correlation of mechanical and electrical properties with processing variables in MWCNT reinforced thermoplastic nanocomposites. *J. Compos. Mater.* 2018; 52: 3681-3697

<https://doi.org/10.1177/0021998318768390>

[46] Ajayan PM, Tour JM. Nanotube composites. *Nature.* 2007; 447: 1066-1068.

<https://doi.org/10.1038/4471066a>

[47] Ghavidel AK, Zadshakoyan M, Kiani G, Lawrence J, Moradi M. Innovative approach using ultrasonic-assisted laser beam machining for the fabrication of ultrasensitive carbon nanotubes-based strain gauges. *Opt Lasers Eng.* 2023; 161: 107325.

<https://doi.org/10.1016/j.optlaseng.2022.107325>

[48] Yang M, Koutsos V, Zaiser M. Interactions between polymers and carbon nanotubes: a molecular dynamics study. *J. Phys. Chem. B.* 2005; 109: 10009-10014.

<https://doi.org/10.1021/jp0442403>

[49] Chen J, Yan L, Song W, Xu D. Interfacial characteristics of carbon nanotube-polymer composites: A review. *Compos. A: Appl. Sci. Manuf.* 2018; 114: 149-169.

<https://doi.org/10.1016/j.compositesa.2018.08.021>

[50] Thi TBN, Ata S, Morimoto T, Okazaki T, Yamada T, Hata K. Visualizing electrical network in microinjection-molded CNT polycarbonate composite. *Carbon.* 2019; 153: 136-147.

<https://doi.org/10.1016/j.carbon.2019.07.019>

[51] Ghavidel AK, Shabgard M, Azdast T. Experimental Study on Oriented Mechanical, Rheological and Optical Properties of Multi-Walled Carbon Nanotubes/Polymethyl Methacrylate Anisotropic Nanocomposite. *Iran. J. Polym. Sci. Technol.* 2016; 29: 249-263.

<https://dx.doi.org/10.22063/jipst.2016.1380>